JOURNAL OF combinatorial CHEMISTRY

Article

Photodegradation Catalyst Discovery by High-Throughput Experiment

Qi X. Dai, Hai Y. Xiao, Wen S. Li, Yan Q. Na, and Xiao P. Zhou

J. Comb. Chem., **2005**, 7 (4), 539-545• DOI: 10.1021/cc049862c • Publication Date (Web): 07 June 2005

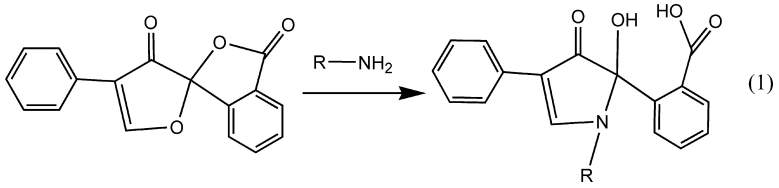

(1)

More About This Article

Additional resources and features associated with this article are available within the HTML version:

- Supporting Information
- Links to the 3 articles that cite this article, as of the time of this article download
- Access to high resolution figures
- Links to articles and content related to this article
- Copyright permission to reproduce figures and/or text from this article

View the Full Text HTML

Journal of Combinatorial Chemistry is published by the American Chemical Society.
1155 Sixteenth Street N.W., Washington, DC 20036

Photodegradation Catalyst Discovery by High-Throughput Experiment

Qi X. Dai, Hai Y. Xiao, Wen S. Li, Yan Q. Na, and Xiao P. Zhou*

Department of Chemical Engineering, Hunan University, China 410082

Received August 13, 2004

A high-throughput experimental methodology was developed for photocatalysis reaction. In this work, a CCD imaging analysis system and photocatalytic reactor for UV light was designed and tested. By making use of the technologies, we have screened several catalyst libraries. From the SiO_2-supported single component catalyst library, we found that TiO_2, ZrO_2, Nb_2O_5, and WO_3 were good candidates for highly active catalyst formulation. We designed and screened several triangle catalyst libraries and found that the WO_3- and Nb_2O_5-codoped TiO_2 catalyst showed much higher photodegradation activities for the degradation of 1,6-hexamethylenediamine than did the pure TiO_2 catalyst. The doping of ZrO_2 into TiO_2 did not generate apparent positive effects on catalytic activity.

Introduction

Since Fujishima and Honda discovered that TiO_2 splits water to hydrogen and oxygen under UV light,[1] a great deal of efforts has been devoted to develop metal oxide semiconductor photocatalysts for air and water purification.[2] A lot of metal oxide semiconductors, such as TiO_2, WO_3, and ZnO were demonstrated to be active photodegradation catalysts.[3−5] Among them, TiO_2 is the most active and also the most widely studied photocatalyst due to its low cost, chemical stability, and nontoxicity. It is because TiO_2 has a band gap of 3.2 eV that the strong oxidation capability of photoexcited holes and OH^- radicals on TiO_2 can oxidize almost all of the organic contaminates in air and water. However, for practical applications, an even higher photocatalytic activity is preferred. Recently, it was reported that by doping TiO_2 with other metal ions, such as adding WO_3 or Al_2O_3 into TiO_2, the photocatalytic activity of TiO_2 was improved.[6] Hence, there might be many opportunities for us to discover photodegradation catalysts by doping TiO_2 with different metal ions. The traditional way of discovering catalysts is to prepare and test catalysts one by one. It could be a big challenge to screen a large number of catalysts. Combinatorial chemistry technology could be a good solution for this problem.

In recent years, the combinatorial chemistry approach has been demonstrated to be a powerful tool for catalyst screening.[7,8] Maier et al. tried to screen photodegradation catalysts by combinatorial chemistry. They successfully developed a photocatalytic reactor and used an automatic HPLC to screen a catalyst library.[7] To further increase the throughput, we developed a high-throughput technology to screen catalysts. In the catalyst preparation, fused silica was used as the support to prepare the catalyst libraries, which can handle milligram levels of catalyst. Our photocatalytic reactor was designed to run more than 100 catalysts simultaneously. The catalysts and reactants were placed in the wells of a polytetrafluoroethylene reactor plate. The wells of the reactor plate were open to the air, which made air diffusion easy; therefore, a gas (air) delivery system was not necessary. This designing makes the reactor construction (described in the Experimental Section) simpler than the traditional photocatalytic reactor, which does need a gas-delivering system. The catalytic activity evaluation is based on the photodegradation of organic reactant. An active photodegradation catalyst should consume more reactant during a certain amount of reaction time. A CCD imaging analysis system was designed to quantify the consumption of organic reactant (in this work, 1,6-hexamethylenediamine was used as the reactant). This CCD imaging analysis system makes it possible to analyze hundreds of samples in a few seconds (see the Experimental Section).

Experimental Section

Preparation of Catalyst Library 1. We selected fused SiO_2 as the support. Since the silica has a very small specific surface area (1.73 m^2/g), the metal compounds coated onto the silica will stay on the surface. Hence, the performance of the catalysts will depend on the properties of the metal compounds on the surface of the silica. In a typical experiment, 10.0000 g of SiO_2 (over 100 mesh) was added into 20.0 mL of ethanol to make a suspension under vigorous stirring, and then 100 μL of the silica suspension (under stirring) was transferred to each glass vessel in the catalyst library to prepare a blank SiO_2 library. Each glass vessel had approximately the same amount of SiO_2.

The precursor solutions of Mn, Fe, La, Na, Pb, Ag, Mg, Co, Ni, Al, Li, K, Bi, Zn, Cr, and Ce were prepared by directly dissolving their nitrate in distilled water. The precursor solution of W was prepared by dissolving $(NH_4)_5H_5$-

* To whom correspondence should be addressed. E-mail: hgx2002@hnu.cn.

10.1021/cc049862c CCC: $30.25
Published on Web 06/07/2005

Table 1. Arrangement of the Catalysts in Catalyst Library 1

Li/SiO_2	Na/SiO_2	K/SiO_2	Mg/SiO_2
Mn/SiO_2	Co/SiO_2	W/SiO_2	Cr/SiO_2
Fe/SiO_2	Al/SiO_2	Ni/SiO_2	Bi/SiO_2
Ti/SiO_2	Zr/SiO_2	Nb/SiO_2	La/SiO_2
Pb/SiO_2	Ag/SiO_2	Ce/SiO_2	Zn/SiO_2

Table 2. Silica-Supported Alkaline Metal Nitrates, Nitrites, and Hydroxides Library

Li/SiO_2[a]	Li/SiO_2[c]
Na/SiO_2[b]	Na/SiO_2[c]
Na/SiO_2[a]	K/SiO_2[c]
K/SiO_2[a]	

[a] The samples were prepared by using $LiNO_3$, $NaNO_3$, and KNO_3 precursors. [b] The sample was prepared by using $NaNO_2$ as precursor. [c] The samples were prepared by using LiOH, NaOH, and KOH precursors.

$[H_2(WO_4)_6]\cdot H_2O$ in distilled water. The precursor solutions of Ti, Nb, and Zr were prepared by dissolving their chlorides in ethanol. The concentration of all the precursor solutions was 0.1 M.

To the above blank SiO_2 library, other metal ion precursor solutions were added according to the following method. For all the precursor solutions, we dispensed 400 μL of solution for each catalyst in the blank SiO_2 library. After we dispensed the precursor solutions into the glass vessels, the vessel holder was shaken to facilitate mixing. The arrangement of the catalysts in library 1 is shown in Table 1. The precursor library was hydrolyzed and dried in air at 48 °C for 1 day to evaporate the solvent and then calcined at 450 °C for 5 h to obtain catalyst library 1 (Table 1).

Preparation of Catalyst Library 2. The blank silica library (2 × 4 elements) was prepared by the same method as that described in the preparation of catalyst library 1. To the blank silica library, 400 μL aqueous solution (0.1 M based on moles of metal) of $LiNO_3$, KNO_3, $NaNO_2$, $NaNO_3$, LiOH, NaOH, or KOH was dispensed into the blank silica library according to the arrangement in Table 2 to obtain a precursor library. The precursor library was dried at 110 °C for 1 day to obtain catalyst library 2.

The Synthesis of the Catalyst Library 3. The Ti precursor was synthesized by dissolving 2.2 mL of $TiCl_4$ in ethanol to make a 40-mL solution under stirring. The Zr precursor was synthesized by dissolving 4.66 g of $ZrCl_4$ in ethanol to make a 40-mL solution under stirring. The W precursor was prepared by adding 5.34 g of $(NH_4)_5H_5[H_2(WO_4)_6]\cdot H_2O$ (particle size was smaller than 100 mesh) in ethanol to make a 40-mL suspension under stirring.

A triangle blank SiO_2 library was synthesized according to the same method described in the synthesis of library 1. To the blank SiO_2 library, Ti, Zr, and W precursor solutions were added according to the concentration formula listed in Table 3; a total solution volume of 1000 μL was maintained in every glass vessel. The dispensing grade of each precursor solution was 100 μL. The precursor library was dried in air at room temperature for 3 days, then at 48 °C for 4 h, then it was calcined at 450 °C for 5 h to obtain triangle catalyst library $TiO_2-ZrO_2-WO_3/SiO_2$. The arrangement of the catalysts in library 3 is shown in Figure 1.

In catalyst libraries 4−6, the Nb precursor was prepared by dissolving 5.41 g of $NbCl_5$ in ethanol to make a 40-mL solution under stirring. The catalysts libraries 4−6 were also synthesized by using the same method as that described in the synthesis of catalyst library 3. The compositions of the catalysts in libraries 3, 4, and 5 are given in the Supporting Information of this paper; the compositions of the catalysts in library 6 are listed in Table 4.

Photodegradation Reaction. The photodegradation reaction was carried out in the photodegradation reactor (Figure 2). The photodegradation reactor included the light box and a reaction plate. The light box had dimensions of 60 × 60 × 60 (cm). There were six medium-pressure mercury UV lamps (each 15 w) installed on the ceiling of the box. The intensity of the UV irradiation at the catalyst library position was 233 $\mu W/cm^2$ (at 254 nm). The reaction plate (16 × 16 × 2 (cm)) was made of polytetrafluoroethylene (PTFE). As shown in Figure 2, a well array was drilled on it (11 × 11 wells; well dimension: i.d. 10 mm, depth 15 mm). These wells act as reaction chambers. When running the reaction, the catalysts were transferred into the wells of the reaction plate, then 600 μL of 1,6-hexamethylenediamine (400 ppm) aqueous solution was dispensed into the wells of the reaction plate, and then the reaction plate containing the reactant (1,6-hexamethylenediamine) solution and the catalysts was kept in the dark for 0.5 h to reach an adsorption−desorption equilibrium. After collecting the starting point data, the reaction plate containing the catalysts and reactant was placed into the light box for the photodegradation reactions.

The CCD Imaging Analysis System. The CCD imaging analysis system was constructed from a CCD camera, two UV lamps, data-collecting software (coming with the CCD camera), data-reducing software (IMGI was made in home), a computer, and a detection box (Figure 3). The CCD camera and UV lamps were installed on the ceiling of the detection box, which had dimensions of 36 × 42 × 50 (cm). To make a uniform intensity distribution of the UV light on the detection plate (area 12 × 15 cm^2) at the bottom of the box, the distance between the UV lamps and the detection plate must be at least 50 cm. The UV lamps are medium-pressure mercury lamps bought from SIM International. The lamps irradiate UV light with a maximum intensity at 365 nm, whereas the lights with other wavelengths are filtrated off by an optical filter (built on the lamps). The CCD camera,-which is monochromatic, was bought from WATEC (Japan, WAT-525EX). The CCD camera has a UV light filter to filter off lights with wavelengths below 400 nm. The spectral response of the CCD camera is given in the Supporting Information. In our case, the fluorescence light excited from the reaction product of 1,6-hexamethylenediamine with fluorescamine had a maximum intensity at 475 nm, which was within the response region of our CCD camera.

The operation of the IMGI software is that after the CCD camera takes a picture, the picture is opened from IMGI. The IMGI will register the light or dark spots of the picture and then integrate the intensity over an individual spot. By this method, if we collected the data of the blank sample data (for us, the background of the PTFE plate), the data of the samples before catalytic reaction, and the data after the

Table 3. Mole Percentage Concentrations of the Components in Triangle Catalyst Libraries 3−5[a]

MO_{n1}	NO_{n2}									
100/0/0	90/10/0	80/20/0	70/30/0	60/40/0	50/50/0	40/60/0	30/70/0	20/80/0	10/90/0	0/100/0
90/0/10	80/10/10	70/20/10	60/30/10	50/40/10	40/50/10	30/60/10	20/70/10	10/80/10	0/90/10	
80/0/20	70/10/20	60/20/20	50/30/20	40/40/20	30/50/20	20/60/20	10/70/20	0/80/20		
70/0/30	60/10/30	50/20/30	40/30/30	30/40/30	20/50/30	10/60/30	0/70/30			
60/0/40	50/10/40	40/20/40	30/30/40	20/40/40	10/50/40	0/60/40				
50/0/50	40/10/50	30/20/50	20/30/50	10/40/50	0/50/50					
40/060	30/10/60	20/20/60	10/30/60	0/40/60						
30/070	20/10/70	10/20/70	0/30/70							
20/080	10/10/80	0/20/80								
10/090	0/10/90									
0/0100										
LO_{n3}										

[a] The formula is mole % M/mole %N/mole % L. The M, N, and L stand for metals.

Table 4. Mole Percentage Concentrations of the Components in Triangle Catalyst Library 6[a]

30% ZrO_2/70% TiO_2										30% WO_3/70% TiO_2
30/0/0	27/3/0	24/6/0	21/9/0	18/12/0	15/15/0	12/18/0	9/21/0	6/24/0	3/27/0	0/30/0
27/0/3	24/3/3	21/6/3	18/9/3	15/12/3	12/15/3	9/18/3	6/21/3	3/24/3	0/27/3	
24/0/6	21/3/6	18/6/6	15/9/6	12/12/6	9/15/6	6/18/6	3/21/6	0/24/6		
21/0/9	18/3/9	15/6/9	12/9/9	9/12/9	6/15/9	3/18/9	0/21/9			
18/0/12	15/3/12	12/6/12	9/9/12	6/12/12	3/15/12	0/18/12				
15/0/15	12/3/15	9/6/15	6/9/15	3/12/15	0/15/15					
12/0/18	9/3/18	6/6/18	3/9/18	0/12/18						
9/0/21	6/3/21	3/6/21	0/9/21							
6/0/24	3/3/24	0/6/24								
3/0/27	0/3/27									
0/0/30										
30% (Nb atomic mol) Nb_2O_5/70% TiO_2										

[a] Only the percentage Numbers of Zr, W, and Nb are listed. The formula is mole % ZrO_2/mole % WO_3/mole % (Nb atomic mol) Nb_2O_5. All of the catalysts in library 6 contain 70% TiO_2.

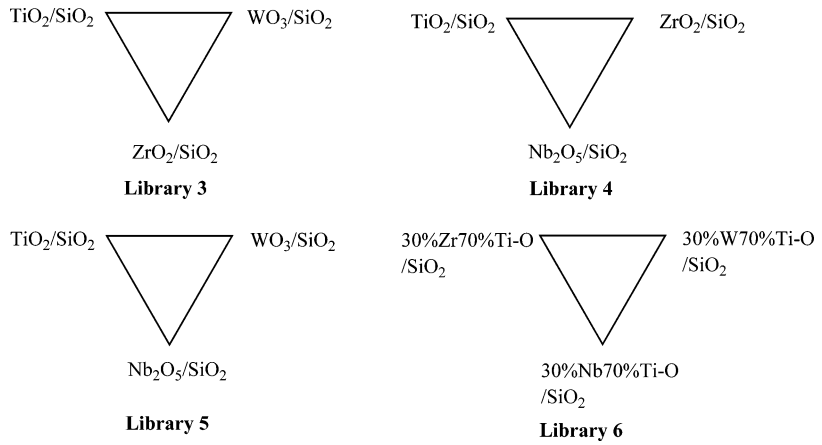

Figure 1. The arrangement of catalysts in triangle catalyst libraries.

catalytic reaction, we could calculate X_i (described in the following section).

The detection plate (Figure 3 right side) was made of PTFEand had dimensions of 12 × 15 × 2 (cm). On the plate, a 12- × 12-well array was drilled. The diameter and depth of every well were 4.0 and 3.0 mm, respectively. The minimum thickness of the wall between every two wells was 1.0 mm.

Quantification. The quantification is based on the measurement of the fluorescence light excited by the reaction product of fluorescamine with primary amine (shown in reaction 1). If amine reacts with fluorescamine, a product will be formed. The product will fluoresce under UV light (365 nm) excitation. The intensity of the fluorescence directly responds to the amount of 1,6-hexamethylenediamine.[9] The CCD camera records the intensity of fluorescence light from sample array by taking pictures.

The picture data is then processed to the software IMGI. IMGI then reads the picture and registers the light spots on the picture and integrates the intensity over individual spots to obtain a data array, which corresponds to the sample array in the detection plate. The detail measurement process and data collecting−reducing process is shown in Scheme 1. As described in the previous section, after the catalysts and reactant solution were transferred to the reaction plate and placed in the dark to reach an adsorption−desorption equilibrium, 30 μL of 1,6-hexamethylenediamine solution was transferred from the wells in the reaction plate to the corresponding wells on the detection plate, and then 30 μL of the fluorescamine solution (800 ppm in DMF) was added

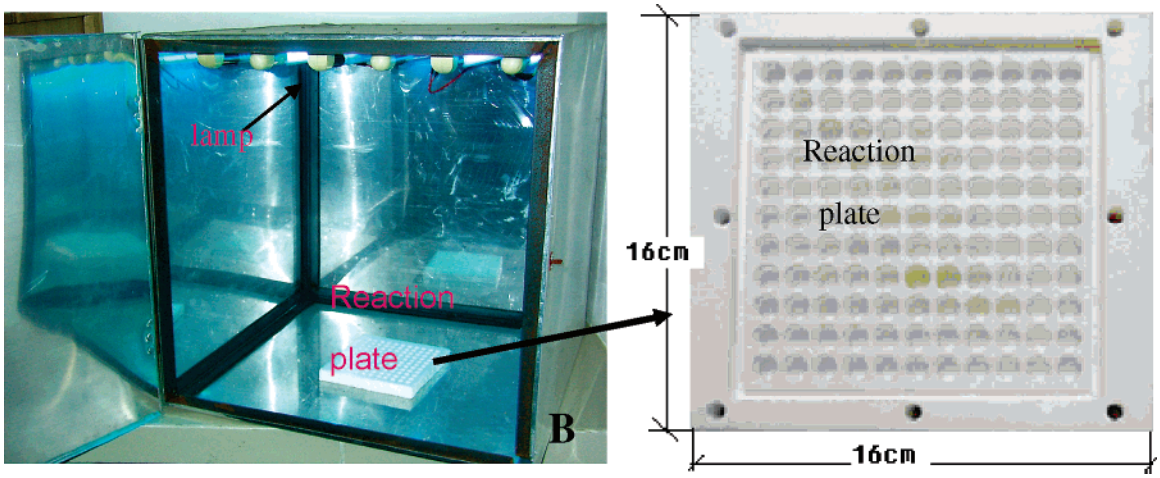

Figure 2. Photocatalytic reactor.

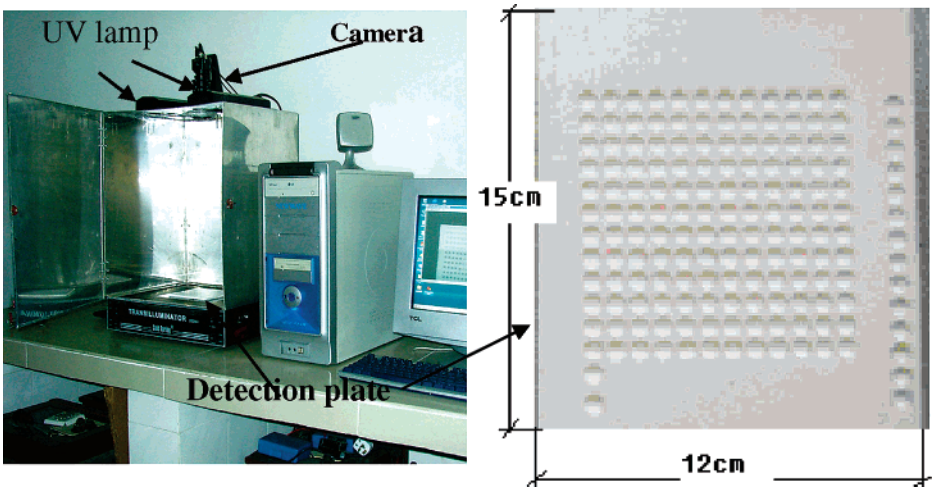

Figure 3. The CCD imaging analysis system.

to every well in the detection plate. After 10 min of reaction, the sample library was analyzed to record the starting point data **B** (a data array.). The reaction plate was placed into the reaction box to carry out the reaction. The analysis can be done at a different period of reaction time, then a data array **C** is obtained. A background data array **A** was taken from a blank detection plate. Since the response is not liner, we define X_i as the appearance conversion. X_i is calculated according to the following method: A_i, B_i, and C_i are the data elements from the corresponding data array of **A**, **B**, and **C** respectively. B_i and C_i are recorded from the same catalyst element i in the catalyst library, and A_i is the background data at the position of the catalyst i. Hence,

$$X_i = (B_i - C_i)/(B_i - A_i)$$

The data flow sheet is shown in Scheme 1. In Scheme 1, an example library was analyzed under our system. X_i is not the conversion number; however, to screen catalysts, X_i can show the conversion variation trend. We can use it to evaluate the relative activities of the catalysts. If necessary, we have home-made calibration software that can convert X_i to conversion numbers, or for secondary scale-up testing, we use GC/MS to analyze the reaction solution. In this work, X_i is not calibrated to the conversion numbers.

The CCD imaging analysis system is very sensitive. It can detect micro- to nanogram-level amine, which is suitable to detect low-concentration contaminants in water and air. Hence, when 1,6-hexamethylenediamine is consumed, the fluorescence will become weaker under UV irradiation. The photodegradation catalysts are evaluated on the basis of the consumption of 1,6-hexamethylenediamine over the catalysts. The control experiment showed a relative analysis error of 4% without catalysts. When catalysts are used, the relative error is within 6%.

The GC/MS analysis was conducted on an Agilent GC/MS 6890N/5973N.

Results and Discussion

GC/MS Analysis of the Samples in the Processing of the Photodegradation Reaction. After the 1,6-hexamethylenediamine aqueous solution was irradiated by UV light over the TiO_2 catalyst, products pent-4-enylamine, 2-methyl-3-aminopropanoic acid, 4-amino-1-butanol, 1-pentanamine, and 1-allylazetidine (these products were confirmed on Agilent GC/MS 6890N/5973N) were detected in the liquid phase (the possible reaction mechanism for the formation of these compounds is suggested in the Supporting Information). Among these products, 2-methyl-3-aminopropanoic acid, pent-4-enylamine, 4-amino-1-butanol, and 1-pentanamine can

Scheme 1. Data Collecting and Reducing Flow Sheet[a]

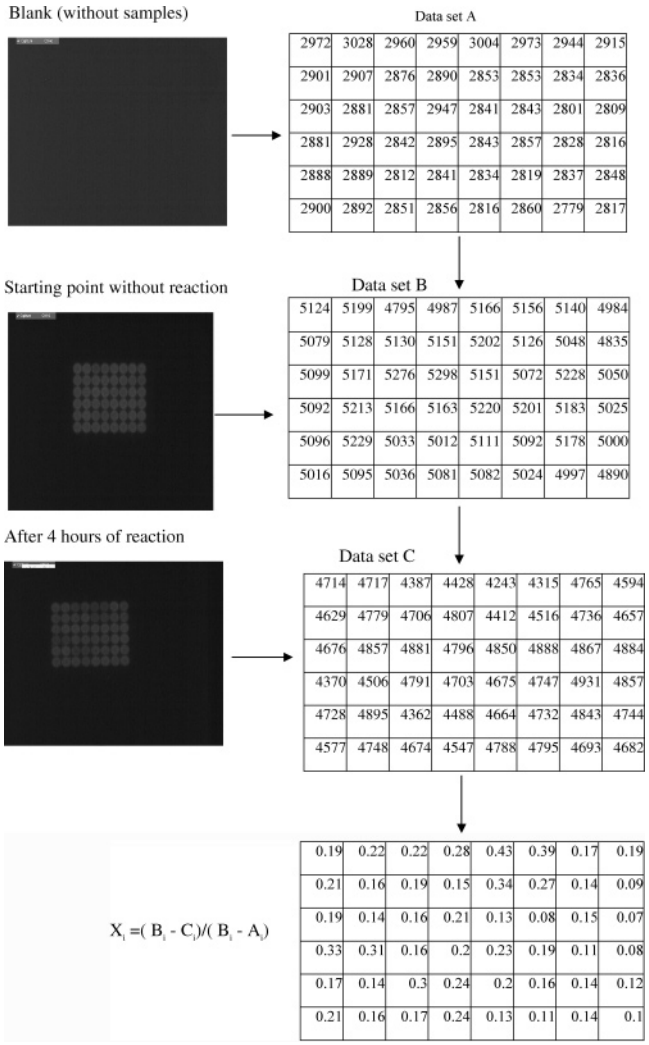

[a] The X_i numbers were automatically caculated by using the software IMGI.

react with fluorescamine to form substances which can generate fluorescence under UV irradiation. However, because of the loss of the amino group, the intensity of the fluorescence will be reduced. Hence, we still detected an intensity decrease in the fluorescence.

The gas-phase sample taken above the reaction plate in the processing of the reaction indicated that there was only N_2, O_2, CO_2, and H_2O in the gas phase (see mass spectra in Supporting Information). We did not find other detectable degradation products of 1,6-hexamethylenediamine. Hence, the gas-phase composition in the light box should not have significant influence on our analysis.

From Figure 4, it can be found that $LiNO_3$, $NaNO_3$, and KNO_3 showed high photodegradation activity to 1,6-hexamethylenediamine in the order of $LiNO_3$ < $NaNO_3$ < KNO_3. The KNO_3 is the most active among the three metal nitrates. It was known that at elevated temperature, the stability of these alkaline metal nitrates has the same order of $LiNO_3$ < $NaNO_3$ < KNO_3. This means that the most stable, KNO_3, should have the highest NO_3^- concentration after calcinations at 450 °C. The reaction was not a catalytic reaction over $LiNO_3/SiO_2$, $NaNO_3/SiO_2$, or KNO_3/SiO_2. This was proved by reactions over library 2. As shown in Figure 5,

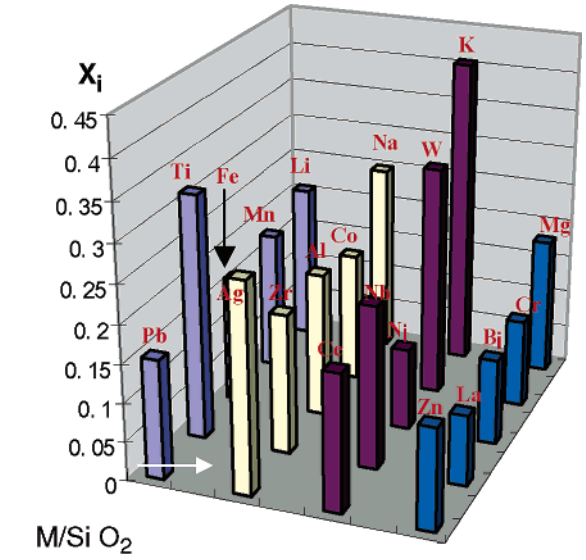

Figure 4. Catalytic reaction results on catalyst library 1 after 4 h of UV irradiation.

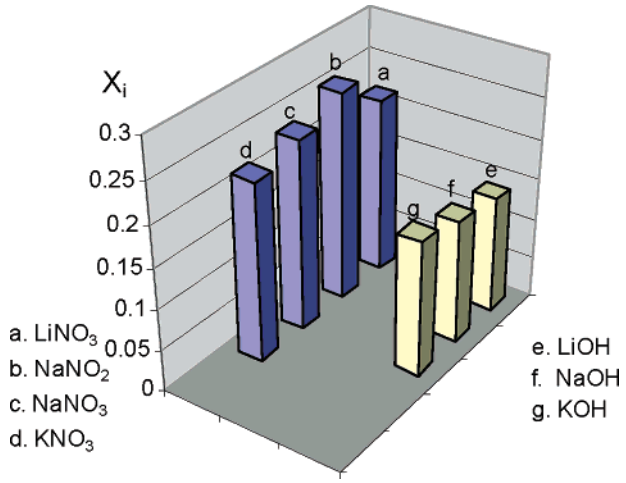

Figure 5. Reaction results on library 2 after 2 h of reaction under UV irradiation.

when $LiNO_3$, $NaNO_2$, $NaNO_3$, KNO_3, LiOH, KOH, and NaOH were supported on silica without calcination, more 1,6-hexamethylenediamine was consumed over $LiNO_3$, $NaNO_2$, $NaNO_3$, and KNO_3 than that over LiOH, NaOH, and KOH. Among the rest of the catalysts, the catalysts TiO_2/SiO_2, WO_3/SiO_2, Ag/SiO_2, Nb_2O_5/SiO_2, and ZrO_2/SiO_2 showed relatively high activity. TiO_2/SiO_2 was the most active catalyst among them. It was well documented that TiO_2 containing catalysts showed high catalytic activities for photodegradation of organic contaminates.[10−12] Martinez et al. reported that 8% SiO_2/TiO_2 was more active and appeared to deactivate more slowly than TiO_2.[13] In our case, the average concentration of TiO_2 in SiO_2 was 6%, which is the revise of the literature report.[14] However, in our case, TiO_2 was coated on a SiO_2 surface, and the surface concentration might still be similar to that reported by Martinez et al. Our case is more likely that the catalysts were actually metal compound-packed silica, since the specific surface area of silica was only 1.73 m^2/g. Dekany et al. reported that ZnO or $Zn(OH)_2$ showed photodegradation catalytic activity in β-naphthol and industrial kerosene mineralization under UV

light.[15] However, the activity is low. This observation is similar to ours. For other metal oxides in catalyst library 1, we have not found many comparable reports. The results in catalyst library 1 indicate that our high-throughput methodology gave reasonable results.

To meet the criteria that the photodegradation catalysts must be stable, nontoxic, and non-water-soluble, we selected TiO_2, WO_3, Nb_2O_5, and ZrO_2 from catalyst library 1 as candidates for further catalyst formulation. Because Ag is a metal (good conductor) and the photocatalyst should be a semiconductor, Ag can only be used as a dopant. The role of Ag in catalyst library 1 might be explained as that in the literature.[16] The dopant silver might act as sites of electron accumulation; this way, better electron−hole separation can be obtained on Ag/SiO_2 particles than on pure SiO_2 particles. Of course, this speculation needs to be proved. In the following work, we designed several ternary triangle catalyst libraries to formulate catalysts.

In triangle catalyst library 3, the data was collected after 4 h of UV irradiation. Among the single-component catalysts TiO_2, WO_3, and ZrO_2, the TiO_2 catalyst showed the highest activity. When doping TiO_2 with ZrO_2, we did not find apparent improvement in the catalytic activity. Yu and Fu et al. reported that ZrO_2/TiO_2 showed higher photocatalytic activity than pure TiO_2;[17,18] however, the improvement was not apparent. Their results are different from ours. However, when WO_3 was added to TiO_2 and the WO_3 concentration was kept below 40%, we saw an apparent improvement in catalytic activities. This is consistent with that reported in the literature.[4,19] Among the WO_3/TiO_2 binary catalysts (do not count in silica), the one containing 20% WO_3 had the highest activity (X_i = 85.7% 1,6-hexamethylenediamine consumption). Among the $TiO_2-WO_3-ZrO_2$ ternary catalysts, none showed higher catalytic activity than 20% WO_3/TiO_2. However, comparing with the catalyst having a composition of 10% WO_3/TiO_2 (X_i = 77.5% 1,6-hexamethylenediamine consumption), the catalyst with a composition of 10% WO_3/10% ZrO_2/TiO_2 showed higher activity (X_i = 84.0% 1,6-hexamethylenediamine consumption).

In Figure 7, the data was collected after 4 h of UV irradiation over catalyst library 4. Pure Nb_2O_5 did not show higher photodegradation activity than pure TiO_2. We found that the catalytic activity variation trend of the ZrO_2-TiO_2 binary catalysts is similar to that in catalyst library 3. We have not observed improvement in catalytic activities over these ZrO_2-TiO_2 catalysts. The results are actually a reproduction of that showed in catalyst library 3. Among the $Nb_2O_5-TiO_2$ binary catalysts, the catalysts containing 20−40% Nb_2O_5 showed high photodegradation activity. The consumption rate of 1,6-hexamethylenediamine over 30% $NbO_{2.5}/TiO_2$ was almost twice that of pure TiO_2. The codoping of ZrO_2 and Nb_2O_5 to TiO_2 did not improve the catalytic activity, as compared with the $Nb_2O_5-TiO_2$ binary catalysts. On the basis of the results of the catalyst libraries 3 and 4, we found that the ZrO_2 doping did not help to improve the catalytic activity of TiO_2; however, the addition of WO_3 or Nb_2O_5 to the TiO_2 made very active photodegradation catalysts. Hence, we have reason to check if we can further improve the catalytic activity by doping TiO_2 with WO_3 and Nb_2O_5. The results can be found in catalyst library 5.

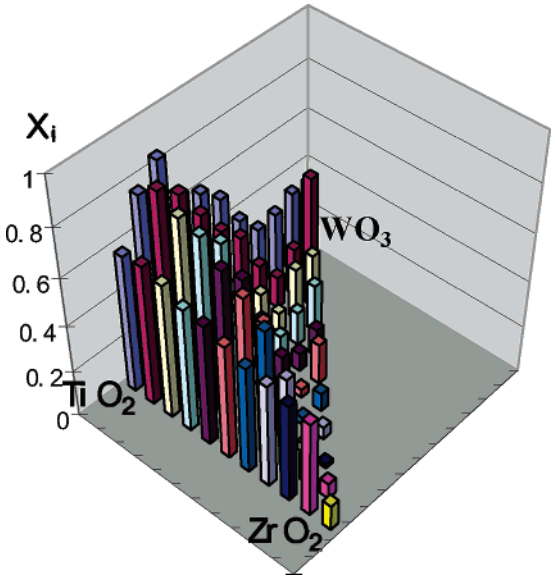

Figure 6. Catalytic reaction results on catalyst library 3 after 4 h of UV irradiation.

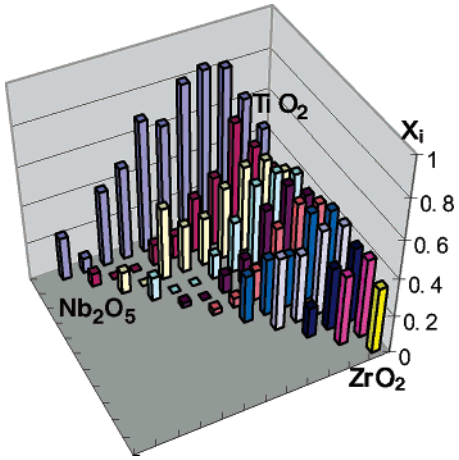

Figure 7. Catalytic reaction results on catalyst library 4 after 4 h of UV irradiation.

For catalyst library 5 after 4 h of UV irradiation, the results are given in Figure 8. Again, we found that among TiO_2, WO_3, and Nb_2O_5, the TiO_2 showed the highest photocatalytic activity. Among the TiO_2-WO_3 binary catalysts, when WO_3 concentration was between 10 and 30%, we observed the highest catalytic activity. Among the $TiO_2-Nb_2O_5$ binary catalysts, the catalysts containing 20−40% Nb_2O_5 showed high activity. From these results, it can be found that the results obtained in libraries 3 and 4 were reproduced in library 5. For the ternary catalysts, the one containing 10% WO_3, 10% (Nb atomic mole) of Nb_2O_5, and 80% TiO_2 and the other one containing 10% WO_3, 20% (Nb atomic mole) of Nb_2O_5, and 70% TiO_2 have the highest catalytic activities. These results indicated that WO_3 and Nb_2O_5 have codoping effects for improving the catalytic activity of TiO_2.

From the results obtained from the above triangle catalyst libraries, we found that WO_3 and Nb_2O_5 have coeffects for improving the catalytic activity of TiO_2, while ZrO_2 did not generate apparent positive effects on the catalytic activity

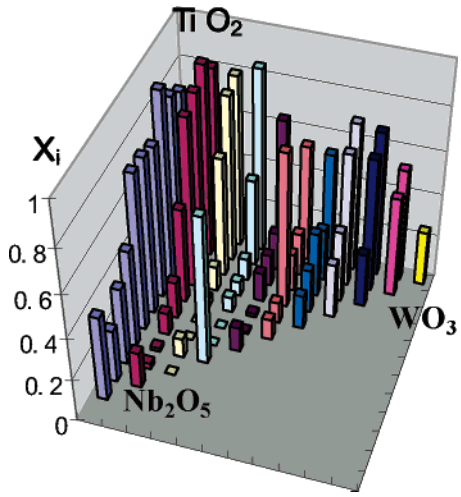

Figure 8. Catalytic reaction results on catalyst library 5 after 4 h of UV irradiation.

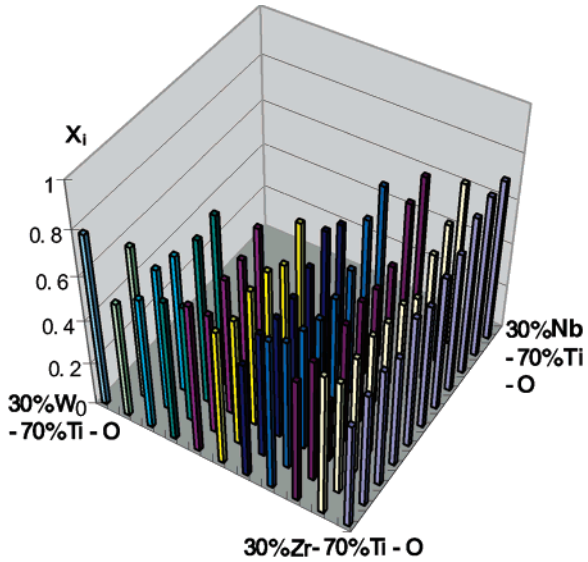

Figure 9. Catalytic reaction results on catalyst library 6 after 4 h of UV irradiation.

of TiO_2. However, we hope to know if ZrO_2, WO_3, and Nb_2O_5 have coeffects for improving the catalytic activity of TiO_2. On the basis of the optimized catalyst compositions in catalyst libraries 3, 4, and 5, we synthesized catalyst library 6 and carried out a photodegradation reaction under the same conditions as those used before. The results are shown in Figure 9. It can be found that ZrO_2 did not show effects on the catalytic activities. The improvement for the catalytic activities came from the doping of Nb_2O_5 and WO_3. The catalysts have compositions of 6−9% WO_3/24−21% $NbO_{2.5}$/70% TiO_2, and 21−24% WO_3/6−9% (Nb atomic mole) Nb_2O_5/70% TiO_2 showed the highest activities. Both of the active composition regions in catalyst library 6 are close to the most active composition regions in catalyst library 5.

Conclusion

Our results indicated that the high-throughput methodology developed by us gave reasonable results. It offered a rapid way to screen photodegradation catalysts for water purification. On the basis of the method, we screened SiO_2-supported single-component metal oxide catalysts and found several potential candidates: TiO_2, ZrO_2, WO_3, and Nb_2O_5. They showed relatively higher photodegradation activities than other catalysts in library 1. Among TiO_2, ZrO_2, WO_3, and Nb_2O_5, TiO_2 showed the highest activity for the photodegradation of 1,6-hexamethylenediamine, which is consistent with that reported in the literature (TiO_2 is a well-documented photodegradation catalyst). We prepared and screened ternary catalyst libraries containing TiO_2, ZrO_2, WO_3, and Nb_2O_5 and found that the addition of ZrO_2 to TiO_2 did not generate positive effects on catalytic activity, but the doping of Nb_2O_5, WO_3, or Nb_2O_5 and WO_3 into TiO_2 greatly improved the catalytic activity of TiO_2.

Acknowledgment. We thank the Nature Science Foundation of China for supporting the project (Project No. 20277008).

Supporting Information Available. Supporting Information as described in the text. This material is available free of charge via the Internet at http://pubs.acs.org.

References and Notes

(1) Fujishima, A.; Honda, K. *Nature* **1972**, *37*, 238.
(2) Yu, J.; Yu, J. C.; Leung, M. K. P.; Ho, W.; Cheng, B. *J. Catal.* **2003**, *217*, 69.
(3) Wu, W.-C.; Liao, L.-F.; Chuang, C.-C.; Lin, J.-L. *J. Catal.* **2000**, *195*, 416.
(4) Fuerte, A.; Hernandez-Alonso, M. D.; Maira, A. J.; Martinez-Arias, A.; Fernandez-Garcia, M.; Conesa, J. C.; Soria, J.; Munuera, G. *J. Catal.* **2002**, *212*, 1.
(5) Szabó, T.; Németh, J.; Dékány, I. *Colloids Surf., A* **2004**, *230*, 23.
(6) Ye, F.; Ohmori, A. *Surf. Coatings Technol.* **2002**, *160*, 62.
(7) Maier, W. F.; Lettmann, C.; Hinrichs, H. *Angew. Chem. Int. Ed.* **2001**, *40* (17), 3160.
(8) Jandeleit, B.; Schaefer, D. J; Powers, T. S; Turner, H. W.; Weinberg, H. W. *Angew. Chem.* **1999**, *111*, 2648.
(9) Desrosiers, P. J.; Dube, C. E.; Zhou, X. P. Worldwide Patent WO 0014529 A1, 2000.
(10) Hoffmann, M. R.; Martin, S. T.; Choi, W.; Bahnemann, D. W. *Chem. Rev.* **1995**, *95*, 69.
(11) Wang, C. Y.; Bahnemann, D. W.; Dohrmann, J. K. *Chem. Commun.* **2000**, 1539.
(12) Mills, A.; Hunte, S. L. *J. Photochem. Photobiol., A* **1997**, *108*, 1.
(13) Mendez-Roman, R.; Cardona-Martinez, N. *Catal. Today* **1998**, *40*, 353.
(14) Lee, G. D.; Jung, S. K.; Jeong, Y. J.; Park, J. H.; Lim, K. T.; Ahnc, B. H.; Hong, S. S. *Appl. Catal., A* **2003**, *239*, 197.
(15) Szabó, T.; Németh, J.; Dékány, I. *Colloids Surf., A* **2004**, *230*, 23.
(16) Vamathevan, V.; Amal, R.; Beydoun, D.; Low, G.; McEvoy, S. *J. Photochem. Photobiol., A* **2002**, *148*, 233.
(17) Yu, J. C.; Lin, J.; Kwok, R. W. M. *J. Phys. Chem. B* **1998**, *102*, 5094.
(18) Fu, X.; Clark, L. A.; Yang, Q.; Anderson, M. A. *Environ. Sci. Technol.* **1996**, *30*, 647.
(19) Song, K. Y.; Park, M. K.; Kwon, Y. T.; Lee, H. W.; Chung, W. J.; Lee, W. I. *Chem. Mater.* **2001**, *13*, 2349.

CC049862C